J. Virol. doi:10.1128/JVI.01723-12

Mutations in the M gene segment can substantially increase replication efficiency of NS1 deletion influenza A virus in MDCK cells.

Running title: Role of M segment in delNS1 influenza replication.

Word count abstract: 243

Word count text: 6298

R. van Wielink [a,b], M.M. Harmsen [a#], D.E. Martens [b], B.P.H. Peeters [a], R.H. Wijffels [b], R.J.M. Moormann [a]

[a] *Central Veterinary Institute of Wageningen UR (CVI), P.O. Box 65, 8200 AB Lelystad, the Netherlands*

[b] *Wageningen University, Bioprocess Engineering, P.O. Box 8129, 6700 EV Wageningen, the Netherlands*

[#] *Corresponding author. Tel: +31 320 238436; fax: +31 320 238668. E-mail address: Michiel.Harmsen@wur.nl*

Abstract

Influenza viruses unable to express NS1 protein (delNS1) replicate poorly and induce high amounts of interferon (IFN). They are therefore considered as candidate viruses for live-attenuated influenza vaccines. Their attenuated replication is generally assumed to result from the inability to counter the antiviral host response, as delNS1 viruses replicate efficiently in Vero cells, which lack IFN expression. In this study, delNS1 virus was parallel passaged on IFN competent MDCK cells, which resulted in two strains that were able to replicate to high virus titres in MDCK cells due to adaptive mutations in especially the M-gene segment, but also the NP and NS gene segments. Most notable were clustered U-to-C mutations in the M segment of both strains and clustered A-to-G mutations in the NS segment of one strain, which presumably resulted from host cell mediated RNA editing. The M segment mutations in both strains changed the ratio of M1 to M2 expression, probably by affecting splicing efficiency. In one virus, 2 amino acid substitutions in M1 additionally enhanced virus replication, possibly through changes in the M1 distribution between the nucleus and the cytoplasm. Both adapted viruses induced equal levels of IFN as delNS1 virus. These results show that the increased replication of the adapted viruses is not primarily due to altered IFN induction, but rather related to changes in M1 expression or localization. The mutations identified in this paper may be used to enhance delNS1 virus replication for vaccine production.

Introduction

The non-structural (NS1) protein of influenza A virus is an antagonist of the cellular antiviral response. Infection with virus either not encoding NS1 protein (delNS1) or encoding a truncated NS1 protein results in high levels of type I interferons (IFN) such as IFN-α or IFN-β. Replication of such viruses is attenuated in IFN competent cell lines, indicating that the NS1 protein is not essential for replication in such hosts (14). In vivo, viruses lacking a fully functional NS1 protein induce IFN in the absence of detectable virus replication (12), which are favourable conditions for use as live attenuated vaccines. The local release of IFN and other cytokines and chemokines appears to be an excellent adjuvant that enhances production of immunoglobulins and contributes to the activation of dendritic cells required for antigen presentation (22, 31). DelNS1 candidate vaccines against influenza A and B have been developed (35, 51) and initial trials in humans showed successful induction of antibody responses (48). Apart from the use in vaccines, delNS1 viruses also show potential as oncolytic agent (27) and viral expression vector (50).

NS1 is expressed at high levels directly after infection and facilitates virus replication in many different ways (reviewed in (15)). Its antiviral properties are focused on reducing the IFN mediated innate immune response and act at several levels. Cytoplasmic dsRNA and 5'-triphosphate-containing RNA are produced during influenza infection and recognized as pathogenic patterns by antiviral proteins like retinoic-acid inducible gene I (RIG-I), dsRNA-dependent protein kinase R (PKR) and 2'-5'-oligoadenylatesynthetase (OAS). NS1 binds both dsRNA and RIG-I, and blocks the activation of PKR and OAS, thereby limiting the onset of several pathways that lead to IFN induction (31). Other functions of NS1 are inhibition of cellular pre-mRNA processing (including IFN pre-mRNA) and mRNA nuclear export (15). Furthermore, NS1 regulates both viral genome replication and translation (49), splicing of M

segment mRNA (32), nuclear export of viral mRNA (13) and viral ribonucleoprotein (vRNP) (49), and viral protein synthesis (7, 10). Recently it was found that NS1 binds the human PAF1 transcription elongation complex (hPAF1C) by a histone-mimicking sequence, thereby inhibiting the role of hPAF1C in the antiviral response (26). NS1 mRNA is transcribed from the eighth vRNA segment. It is partially spliced to generate mRNA that encodes the nuclear export protein (NEP) (15). In the nucleus of infected cells, NEP facilitates the export of the vRNP complexes containing the viral genome segments to the cytoplasm, where assembly of the viral components is completed before virus budding takes place (1). Independent from vRNP export, NEP also regulates viral genome transcription and replication (33). During development of delNS1 strains it is therefore essential to retain the NEP protein.

In cells and animals with a low or absent IFN response, such as Vero cells, STAT1 or PKR knock-out mice, delNS1 virus replicates to high titres (8, 14, 20), whereas replication is attenuated in MDCK cells and other IFN-competent hosts. When Vero cells are externally stimulated with IFN-α before infection, delNS1 virus replication is however also attenuated (12). Moreover, delNS1 only replicated efficiently in embryonated chicken eggs younger than 8 days, when the host immune response is not yet fully developed (43). It is therefore generally assumed that the inability of delNS1 virus to counter the cellular innate immune response is the major cause for its attenuated phenotype (31). In addition to the unimpaired IFN response, the absence of NS1 during influenza virus infection results in enhanced apoptosis induction (41, 57). Activation of caspases, a group of cysteine proteases that play an important role in apoptosis, results in cleavage of viral NP protein and thereby limits the amount of viral protein available for assembly of viral particles (56). The antiviral effect of apoptosis is therefore believed to contribute to the attenuated replication of delNS1 virus. Inhibition of the apoptotic response is attributed to both the activation by NS1 of the

phosphatidylinositol 3-kinase (PI3K)-Akt signalling pathway, which is known to result in an anti-apoptotic response (9, 55), as well as the inhibition of IFN. IFN sensitizes cells for apoptosis (57) through its transcriptional induction of PKR (44) and activation of the FADD/caspase-8 death signalling pathway (4). The role of apoptosis in influenza infection is, however, still uncertain as several influenza proteins, including NS1, also exhibit pro-apoptotic functions. Furthermore, influenza virus replication is impaired in the presence of caspase inhibitors (52), which appears to be caused by retention of vRNA complexes in the nucleus, preventing formation of progeny virus particles. A possible explanation for this double role of NS1 in apoptosis regulation could be prevention of cell death by inhibition of apoptosis early in the infection, followed by induction at a later stage (55). Ludwig et al. (24) suggested that caspases enhance vRNP export from the nucleus later in the infection by widening of the nuclear pores, thereby allowing diffusion of vRNP out of the nucleus.

Previously we showed that delNS1 virus can efficiently be propagated on a MDCK cell line showing inducible expression of NS1 from a trans-complementing genomic gene (46). A 500-fold increase in infectious virus titre was observed, even though the NS1 level was 1000-fold lower than that in cells infected with wild-type (WT) virus. Furthermore, apoptosis was reduced to similar levels as found in WT virus infected cells, whereas the induction of IFN by delNS1 virus was not significantly reduced in these cells. Because of the limited effect on IFN induction, we then hypothesized that the low yield of delNS1 virus on normal MDCK cells could be caused by loss of another NS1 regulatory function rather than the inability of the virus to interfere with the host cells antiviral response. In this paper we increased the replication efficiency of delNS1 virus by adaptation to IFN competent MDCK cells during serial passage. Next, we determined if the observed increase in virus yield was related to decreased IFN and apoptosis induction. Furthermore, we identified the mutations

112 and partly characterized the mechanism that allowed the virus to efficiently replicate in the
113 absence of the NS1 protein.
114

Materials and methods

Cell culture and virus strains

MDCK-SFS (Serum-Free Suspension) cells (47) were grown in suspension in SFM4BHK21 medium (Hyclone, Waltham, MA), supplemented with 8 mM glutamine, 5 mg/L phenol red and 1.5 g/L sodium bicarbonate, or adherent in serum-free UltraMDCK medium (Lonza Biowhittaker, Basel, Switzerland) supplemented with 4 mM glutamine. Adherent NS1Bon2 MDCK cells (46) were also grown in UltraMDCK medium, additionally supplemented with 200 µg/ml G418 (Promega, Fitchburg, WI) and 100 µg/ml hygromycin B (Clontech, Mountain View, CA). G418 and hygromycin were not used during virus infections. Vero and Human embryo kidney (293T) cells were cultured in Glutamax medium (Invitrogen, Carlsbad, CA) supplemented with 10% FBS. All culture media were provided with 100 units/ml penicillin and 100 µg/ml streptomycin (Gibco). Cells were grown at 37˚C and 5% CO_2. Suspension cells were grown in shaker flasks at 100 rpm. Cell density and viability were determined with a Countess automated cell counter (Invitrogen).

All virus strains described in this paper are based on the A/PR/8/34 [H1N1] (PR8) strain in which the HA and NA genes are replaced by those from A/turkey/Turkey/1/05 H5N1 (46). The multi-basic cleavage site of H5 was replaced by that of a low pathogenic H6 subtype (46) and we refer to this HA gene segment as H5(6). This H5(6)N1 virus (46) strain containing the complete NS segment was passaged once in 9-day old embryonated eggs after virus rescue, and is referred to as WT virus. The influenza delNS1 virus strain (46) used for the adaptation to MDCK-SFS cells is isogenic to WT virus except for the NS gene segment. It was previously passaged 10 times in 7-day old embryonated chicken eggs and is referred to as delNS1^{EA}. Note that in the comparison of reassortant virus replication, protein expression, apoptosis and IFN-induction, a non-adapted delNS1 virus strain was used, to

which we refer as delNS1. The infectious influenza virus titre was measured by determining the tissue culture infective dose required to infect 50% ($TCID_{50}$) of MDCK cells, as previously described (47). All virus strains were propagated on the NS1 expressing NS1Bon2 MDCK cell line to generate virus seed stocks with high infectious virus titres (>7 log10 $TCID_{50}$/ml) prior to further viral characterization. For this purpose, NS1 expression was induced in this cell line 24 h before infection by addition of 1 µg/ml doxycycline (Clontech) to the culture medium, followed by infection at multiplicity of infection (MOI) 0.01 and harvesting at 3 days post-infection (dpi).

Virus adaptation

Two independent adaptation experiments were performed. In the first experiment, MDCK-SFS cells in suspension were infected with delNS1^{EA} at MOI 0.1. After 2-3 days the supernatant was collected and a 500-fold dilution was used for subsequent infection of fresh MDCK-SFS cells (unknown MOI). The virus was serially passaged 10 times in this manner. In the second adaptation experiment 5 serial passages were performed, starting with infection of adherent MDCK-SFS cells with delNS1^{EA} at MOI 0.01. The infectious virus titre was determined daily and the supernatant with the highest titre was used in subsequent infection of fresh MDCK-SFS cells at MOI 0.01. The two adapted virus strains were cloned 3 times by limiting dilution on MDCK-SFS cells. Of each adapted strain, eight clones were screened for virus replication on MDCK-SFS cells and one clone of each strain with high titre was selected and amplified on NS1Bon2 cells. The resulting strains are referred to as delNS1^{CA1} and delNS1^{CA2} respectively.

Plasmids

Ten plasmids containing single or multiple mutations found in delNS1^{CA1} and delNS1^{CA2} (Table 1) were made. Viral RNA of delNS1^{CA1} and delNS1^{CA2} was isolated from seed virus and HA and M gene segments were amplified by PCR, using primers with BsmBI restriction sites (18). The resulting cDNAs were inserted in plasmid pHW2000 to create pROM33-pROM36. Plasmids containing the mutated PB1 segments of delNS1^{CA1} and delNS1^{CA2} could not be made. pROM16 was made by cloning a synthetic 675 bp BsrGI-NgoMIV fragment (GenScript Corporation, Piscataway, NJ) containing mutation A1381G in pHW195 containing the PR8 NP gene (17). Synthetic fragments with suitable BsmBI restriction sites comprising the complete M segment with one or more of the CA2 mutations or the complete delNS1 NS segment with all six CA1 mutations were inserted in pHW2000 to construct pROM13 and pROM51-pROM54. All plasmid inserts were sequenced to ensure the absence of additional nucleotide substitutions.

Rescue of recombinant influenza virus

To generate recombinant influenza virus, a mixture of 1.5 x 10^6 293T and 5 x 10^5 MDCK-SFS cells were transfected with equal amounts of the eight plasmids containing the different gene segments, using Fugene HD (Roche Applied Science, Penzberg, Germany). DelNS1 viruses were made using plasmids pHW191 (GenBank accession no. of vRNA coding region: AB671295), pHW192 (EF467819), pHW193 (CY058518), pHW195 (EF467822), pHW197 (EF190985) (17), pPolsaprib H5, pPolsaprib N1 and pHW NEP (46), whereas WT virus was made by replacing pHW NEP with pHW198, which contains the full length NS segment. All other recombinant viruses were made by replacing one or more plasmids with those in Table 1. At 24 h post-transfection (hpt) the transfection mixture was replaced by

Glutamax medium supplemented with 0.3 % bovine serum albumin (Chemie Brunschwig AG, Basel, Switzerland) and 1 µg/ml TPCK-trypsin (Sigma-Aldrich, St. Louis, MO). Virus was harvested at 96 hpt. Virus stocks were generated using NS1Bon2 cells as described above and virus identity was confirmed by sequence analysis. Reassortant delNS1 virus strains are referred to as delNS1, followed by the mutated gene segment(s) it contains (Table 1) and the adapted virus from which they originate (e.g. delNS1:[NP M]^{CA1}, which contains the mutated NP and M gene segments from delNS1^{CA1}).

Virus genome sequencing

Viral RNA genomes were isolated using a high pure viral RNA isolation kit (Roche Applied Science). Universal influenza genome primer uni12 (18) was used for reverse transcriptase reactions with the Superscript III first strand synthesis system (Invitrogen), followed by segment specific PCR reactions with an Expanded high fidelity PCR system (Roche Applied Science). DNA sequencing was performed at Baseclear (Leiden, the Netherlands) and sequence analysis was done with Lasergene (DNASTAR Inc, WI).

Comparison of virus replication

To study the infection kinetics of the different virus strains, 10^6 MDCK-SFS or Vero cells per well were incubated in 6-well plates, in 5 ml UltraMDCK medium containing 2 µg/ml trypsin-TPCK. Cells were infected in triplicate at MOI 0.01. Because of their ability to inactivate trypsin (19), Vero cells were supplied with additional trypsin-TPCK (1 µg/ml) at 24 and 48 hour post-infection (hpi). Supernatant was sampled at the indicated intervals and stored at -80°C before determining the infectious virus titre.

The main effect and interactions of the mutated gene segments on the infectious virus titre was analysed by a repeated measures ANOVA with data from two infection experiments, both performed in triplicate, using R statistical software package (R Foundation for Statistical Computing, Vienna, Austria). Analysis was performed separately for delNS1^{CA1} and delNS1^{CA2} reassortants datasets, with the mutated gene segments as explanatory variables, the two infection experiments as random effects and delNS1 virus as the baseline. Non-significant explanatory variables were excluded from the model.

IFN reporter assay

MDCK-SFS cells were allowed to attach to the surface of eight 96-well plates for 1 h (4.5×10^4 cells/well) and then transiently cotransfected with a reporter plasmid carrying a firefly luciferase gene under control of the IFN-β promoter (p125Luc, kindly provided by Takashi Fujita, Kyoto University, Japan (54) and a Renilla luciferase control plasmid pGL4.73 (Promega), using Fugene HD. The next day, supernatant was removed and cells were infected in triplicate (MOI 5) with WT, delNS1, delNS1^{CA1}, delNS1^{CA2}, delNS1:M^{CA1}, delNS1:M^{CA2} or delNS1:M$^{CA2.3}$, or mock infected. One hour later, supernatant was replaced with fresh medium. At 9, 12, 16, 20 and 24 hpi one plate was stored at -20˚C without supernatant. The firefly luciferase activity of all plates was measured with a GloMax-Multi luminometer (Promega) using the Dual Luciferase Reporter Assay System (Promega) and normalized to the Renilla luciferase activity.

Apoptosis assay

MDCK-SFS cells were allowed to attach to the surface of six 96-well plates for 1 h (10^4 cells/well) and infected in sextuple with WT, delNS1, delNS1^{CA1} or delNS1^{CA2} virus (MOI 5),

or mock infected. One hour later, supernatant was replaced with fresh medium. At 10, 14, 16, 19, 22 and 26 hpi, one plate was stored at -20˚C without supernatant. Apoptosis was determined by the activity of caspase-3 and caspase-7 using Caspase-Glo 3/7 Assay (Promega). Caspase-Glo reagent, diluted 1:1 with PBS, was added to the frozen cells (50 µl/well). After 1.5 h incubation at room temperature, the luminescence was measured with a GloMax-Multi luminometer.

Western blot analysis of M1 and M2 expression

MDCK-SFS cells were allowed to attach to the surface of 24-well plates for 1 h (3.3 x 10^5 cells/well) and infected (MOI 5) or mock infected, in triplicate. HEK293T cells (10^6 cells/well in 6-well plates) were transiently transfected in triplicate, using Fugene HD with either 2 µg/well pHW195, pROM35, pROM36, pROM51, pROM52, pROM53, pROM54 (Table 1) or mock transfected. At 10 hpi or 48 hpt, cells were lysed with reducing NuPAGE sample buffer containing in addition complete EDTA-free protease inhibitor cocktail (Roche). Samples were sheared with a 21G needle, incubated for 10 min at 75°C and loaded onto NuPAGE® Novex® 12% Bis-Tris precast gels (Invitrogen). Polypeptides were transferred to polyvinylidenedifluoride membranes and detected by immunoblotting using monoclonal mouse antibodies (Santa Cruz Biotechnology, Santa Cruz, CA) against M1 (SC-57881, 0.2 µg/ml) or M2 (SC-32238, 0.4 µg/ml). After subsequent incubation with peroxidase-conjugated rabbit anti-mouse immunoglobulins (0.13 µg/ml; Dako, Glostrup, Denmark), proteins were visualized with ECL plus (GE Healthcare, Buckinghamshire, UK) and quantified with a Storm840 imaging system and ImageQuant software (Molecular Dynamics, Sunnyvale, CA). The M1/M2 band intensity ratio of each sample was calculated before determining the mean ratio of the triplicate infections or transfections.

Subcellular M1 localization

MDCK-SFS cells were cultured in suspension (6.6 x 10^5 cells/ml) and infected with WT, delNS1 or delNS1:$M^{CA2.3}$ in triplicate (MOI 5). At 6 and 10 hpi, 10^6 cells were harvested and cytoplasmic and nuclear extracts were prepared with the NE-PER nuclear and cytoplasmic extraction kit (Thermo Fisher Scientific, Rockford, IL), according to the manufacturer's description. However, complete EDTA-free protease inhibitor cocktail was added to the extraction reagents. Cytoplasmic and nuclear extractions were subjected to reducing SDS-PAGE and Western blot analysis as described above. Polypeptides were detected by immunoblotting as described in the previous section with monoclonal mouse antibodies (Santa Cruz Biotechnology) against lamin A/C (SC-7292, 0.2 µg/ml), tubulin (SC-5286, 0.2 µg/ml) or M1 (SC-57881, 0.2 µg/ml). Cytoplasmic and nuclear specific proteins tubulin and lamin A/C were used to assess the purity of nuclear and cytoplasmic extracts. The amount of M1 protein was corrected for the extraction efficiency by either tubulin (cytoplasmic extracts) or lamin A/C (nuclear extracts). The ratio of corrected nuclear M1 to corrected cytoplasmic M1 was calculated before determining the mean ratio of the triplicate infections.

Results

delNS1 virus adaptation

The egg-adapted influenza virus delNS1^{EA} replicated poorly in MDCK cells, reaching a maximum infectious virus titre that was 10^4-fold lower than that of WT virus (Fig. 1B). To investigate whether the virus was able to overcome the negative effect of the NS1 deletion by acquiring compensating mutations we serially passaged delNS1^{EA} virus on MDCK-SFS cells in two independent adaptation experiments (see Materials and Methods). In the first cell adaptation experiment (CA1), virus was blindly passaged 10 times. In the second experiment (CA2), virus taken from the time point where the titre was maximal was used to infect cells in the next passage at a controlled MOI of 0.01. Both adaptation experiments on MDCK-SFS cells resulted in virus populations with increased replication rate and increased maximum titres compared to the parent strain. The maximum virus titre of strain delNS1^{CA2} increased during the first 3 to 4 passages, but did not increase further during the fifth passage (Fig. 1A). To obtain clonal virus, the adapted strains were further cultured during 3 limiting dilution steps on MDCK-SFS cells. The infectious virus titres of the resulting cloned cell-adapted virus strains delNS1^{CA1} and delNS1^{CA2} were about 250-fold higher than the parental delNS1^{EA} virus titre, but remained 25-fold lower than the WT virus titre (Fig. 1B). In Vero cells, delNS1^{EA} was only weakly attenuated in comparison to the WT virus (Fig. 1C). Adaptation of delNS1 virus to MDCK-SFS cells caused only a small increase in delNS1^{CA2} virus replication in Vero cells whereas delNS1^{CA1} virus replication was comparable to the parental delNS1 virus (Fig. 1C). Thus, the increase in virus replication due to virus adaptation is much higher during propagation on MDCK-SFS cells as compared to Vero cells.

Sequence analysis of adapted virus

All eight gene segments of the delNS1^{CA1} and delNS1^{CA2} virus strains and their parental delNS1^{EA} strain were sequenced (Table 2). No mutations were found in the PB2, PA and NA segments. The delNS1^{EA} virus contained two mutations in PB1 and one in HA with all mutations present in approximately 50% of the virus population. These mutations were silent and must have arisen during the passaging in eggs. Both PB1 mutations were present in both cell adapted viruses, whereas the HA mutation was only present in delNS1^{CA2} virus. Due to the presence of mutations in the delNS1^{EA} virus, a non-adapted delNS1 virus was used in the comparison of reassortant virus replication, protein expression, apoptosis, and IFN-induction experiments. We refer to this virus as delNS1.

Compared to delNS1^{EA} virus, delNS1^{CA1} virus had 13 additional mutations, including a silent mutation in PB1, F257L in HA, R446G in NP, four silent U-to-C mutations in M, and six A-to-G mutations in the delNS1 segment. Three of the NS segment mutations resulted in the amino acid substitutions Y41C, M52V and I76V in the NEP protein. The first 4 A-to-G mutations in the NS^{CA1} segment are located on the part that normally encodes NS1, resulting in two amino acid substitutions at the NS1 C-terminal. These mutations may be disadvantageous to the WT virus and removal of the NS1 ORF therefore increased the freedom of this segment to acquire mutations. DelNS1^{CA2} virus had 6 additional mutations that were all located in the M segment. These mutations started to appear simultaneously at passage 4 and had increased at passage 5 (Fig. 2A). Again, these 6 mutations were all U-to-C mutations, two of which resulted in amino acid changes V97A and Y100H in M1. Notably, all mutations on the M and NS segments are clustered in regions of 50-100 nucleotides. Both M segment mutation clusters are located on a region of the M1 mRNA that is removed by splicing to generate the M2 mRNA and thus do not affect M2 mRNA

structure (Fig. 2B). Apart from the two silent mutations in PB1 which were already present in the initial delNS1^{EA} virus, both parallel adaptations did not lead to identical mutations.

Infection with delNS1 viruses containing mutated gene segments

The effect of each mutated gene segment on the infectious virus titre, and possible interactions between the gene segments was determined by employing a full-factorial analytical approach. MDCK-SFS cells were infected with reassortant delNS1 viruses consisting of all 15 possible combinations of delNS1^{CA1} virus HA, NP, M and NS gene segments, or the 3 possible combinations of delNS1^{CA2} virus HA and M gene segments (Fig. 3A). All reassortant viruses contained the WT PB1 segment, as we were unable to generate plasmids containing the mutated PB1 segments. Infectious virus titres were examined using a repeated measures ANOVA, so as to determine the relative importance of the gene segments, and possible interactions between gene segments, on virus replication. Segments with significant effect on the delNS1^{CA1} virus titre were NS^{CA1}, M^{CA1} and NP^{CA1}, with coefficients of respectively 0.68, 0.76 and 0.50 (all $p<0.001$). These coefficients specify the average increase of the virus titre in $\log^{10}$ $TCID_{50}$/ml, when the mutated segment was included in the delNS1 reassortant strain. There was also an interaction effect between the mutated M and NP segments of -0.36 ($p<0.05$), which indicated an average decrease in virus titre when the mutated M and NP segments were combined in the delNS1 virus. Thus, the enhanced delNS1^{CA1} virus replication was the effect of these three mutated gene segments together. The enhanced replication of delNS1^{CA2} was determined by the mutated M segment alone (Fig. 3A). This observation was confirmed by statistical analysis, which appointed a coefficient of 2.0 ($p<0.001$) to M^{CA2}, indicating that the 100-fold increase in virus titre was solely determined by the M segment mutations. Reassortant virus containing

all mutated gene segments (delNS1:[HA NP M NS]^{CA1} and delNS1:[HA M]^{CA2}) replicated equally well as the virus from which their segments originated, delNS1^{CA1} and delNS1^{CA2}, indicating that the mutated PB1 gene segments did not contribute to the enhanced virus replication.

Because the M segment plays a major role in increased replication of both adapted viruses, we further focused on the mechanism by which mutations in this segment could overcome the decreased replication in the absence of NS1. To determine which individual M^{CA2} mutation was responsible for virus titre increase, four additional mutant virus strains were made containing either the V97A or Y100H mutation, the combination of V97A and Y100H, or the remaining four silent mutations (Fig. 3B). When compared to delNS1, the two strains with single amino acid substitutions did not replicate more efficiently. However, when V97A and Y100H were combined in delNS1:M$^{CA2.3}$, a 50-fold increase in virus titre was observed. Furthermore, the four silent mutations increased the virus yield approximately 10-fold, as indicated by the comparison of delNS1 to delNS1:M$^{CA2.4}$ and delNS1:M$^{CA2.3}$ to delNS1^{CA2}. Interestingly, when introduced into the WT virus, the M^{CA2} segment decreased replication (Fig. 3B).

Interferon-β and apoptosis induction by cell adapted delNS1 virus

To assess if viral adaptation affected IFN-β expression, cells were transfected with a firefly luciferase reporter gene under control of an IFN-β promoter and subsequently infected with WT or different delNS1 virus strains at high MOI. The low luciferase activity of cells infected with WT virus as compared to cells infected with delNS1 virus indicates inhibition of IFN-β induction by NS1 (Fig. 4A). Both cell-adapted viruses (Fig. 4A) as well as delNS1 reassortant virus containing either M^{CA1}, M^{CA2} or the M segment containing the two

CA2 amino acid mutations (Fig. 4B) did not show lower IFN induction than parental delNS1 virus (Fig. 4A). This indicates that the increase in virus replication due to virus adaptation was not caused by a lower IFN induction.

The induction of apoptosis was determined by measuring the activity of caspase-3 and caspase-7, two proteases that are induced late in the apoptosis pathway. Again, the inhibiting effect of NS1 was visible as little caspase activity was seen in cells infected with the WT virus in comparison to cells infected with delNS1 viruses. Both cell-adapted delNS1^{CA1} and delNS1^{CA2} viruses similarly induced caspase activity to a level that is far higher than observed with WT virus (Fig. 4C).

Effect of M segment mutations on M1 and M2 protein expression

To determine if the M segment mutations affected splicing of the M1 mRNA (Fig. 2B) we measured the ratio of M1 and M2 protein expression in cells at 10 hpi by Western blot analysis (Fig. 5A). The M1 protein of all Y100H mutant viruses (delNS1:M^{CA2}, delNS1:M$^{CA2.2}$ and delNS1:M$^{CA2.3}$) migrated slightly slower in SDS-PAGE than that of the other virus strains (Fig. 5A, lanes 4, 6 and 7 respectively). Slight changes in mobility in SDS-PAGE due to amino acid changes that affect protein charge, such as Y100H, have been observed before (30).

Cells infected with delNS1 virus (Fig. 5A, lane 2) appeared to express more M2 protein than WT virus infected cells (Fig. 5A, lane 1). This difference was consistently observed in several experiments, even though the difference in M1/M2 ratio was not statistically significant from that of the WT virus (Fig. 5B). Infection with virus containing the mutated M segments, delNS1:M^{CA1} (Fig. 5A, lane 3) and M^{CA2} (Fig. 5A, lane 4), resulted in an M1/M2 ratio that was 2- and 3-fold higher, respectively, than that of delNS1 (Fig. 5B). Virus containing only the single or double M1 amino acid mutations (delNS1:M$^{CA2.1}$, M$^{CA2.2}$ and

394 $M^{CA2.3}$, Fig. 5A lanes 5, 6 and 7) showed an M1/M2 ratio similar to delNS1, whereas
395 delNS1:$M^{CA2.4}$ virus (containing the 4 silent M^{CA2} mutations) showed a 2-fold increase (Fig.
396 5A lane 8 and Fig. 5B). The effect of the mutations on M1 and M2 expression was confirmed
397 by transfection of HEK293T cells with plasmids encoding the different M segments (Fig. 5C).
398 The M1/M2 ratio of cells transfected with WT M segment (0.35; Fig. 5D), is comparable to
399 that of delNS1 infected cells (0.42; Fig. 5B). The M1/M2 expression ratio was higher with
400 segments containing the original mutations acquired during the adaptation (M^{CA1} and M^{CA2})
401 and with the M^{CA2} segment containing the four silent mutations ($M^{CA2.4}$; Fig. 5C lanes 3, 4
402 and 8), but not with the M^{CA2} segments containing one or both of the non-silent mutations
403 (Fig. 5C lane 5, 6 and 7). Taken together, these results show that both cell-adapted viruses
404 acquired mutations that increased the M1/M2 protein ratio in infected cells.
405
406 **Effect of M1 amino acid substitutions on subcellular localization**
407 The M1 mutations V97A and Y100H present in delNS1^{CA2} are located close to the NLS
408 at position 101-105 (Fig. 2C). To determine whether they affected the subcellular
409 localization of M1 protein, cells were infected with WT, delNS1 or delNS1:$M^{CA2.3}$ virus and
410 the nucleoplasm and cytoplasm was isolated early (6 hpi) and late (10 hpi) in the infection
411 process. The level of M1 present in both compartments was then determined by Western
412 blot analysis and quantified by phosphorimager densitometry (Fig. 6A and B).
413 At 6 hpi, the ratio of nuclear to cytoplasmic M1 was comparable between WT and
414 delNS1 virus infected cells (Fig. 6B). Four hours later, this ratio remained constant in WT
415 virus infected cells whereas it was 4-fold lower in delNS1 virus infected cells, mainly due to a
416 decrease in nuclear M1. Thus, NS1 appears to affect the concentration of M1 in the nucleus
417 late but not early in the infection. The mutant virus containing only M1 amino acid

418 substitutions V97A and Y100H showed a higher ratio at early stages, although this did not
419 significantly differ from the ratio of the other two viruses. At 10 hpi nuclear M1 was not
420 detectable anymore, thereby reducing the localization ratio below that of delNS1 infected
421 cells.
422

Discussion

The low yield of delNS1 virus on MDCK cells is assumed to be caused by the inability of this virus to inhibit the antiviral host response (14). In this study, we obtained two delNS1 influenza virus variants that replicated to 250-fold higher infectious virus titres ($TCID_{50}$) after two parallel, serial passages on MDCK cells. However, the increase in virus replication did not correlate with a lower induction of IFN or apoptosis, which is linked to IFN induction (4, 44, 57). These results thus indicate that IFN induction may not be the only cause of limited delNS1 virus replication in MDCK cells. Several recent studies already suggest that IFN has a minor effect on influenza replication in MDCK cells because canine myxovirus resistance proteins lack anti-influenza activity (38) and secreted IFN is proteolytically degraded by trypsin, which is normally present during influenza production on MDCK cells (39). Furthermore, delNS1 virus titres could be increased by recombinant NS1 expression, without lowering IFN induction (46), indicating that IFN induction in MDCK may play a less important role than generally assumed.

The two adapted viruses contained a high frequency of either A-to-G or U-to-C substitutions (19 out of 22) that occur mostly (16 out of 22) in three clusters in M^{CA1}, M^{CA2} and NS^{CA1} gene segments. Furthermore, all mutations in M^{CA2} appeared to be acquired at the same time. Taken together, this suggests that these substitutions result from hyperediting by adenosine deaminases acting on RNA (ADAR), which cause A-to-G substitutions in RNA (37). Hyperediting of the influenza genome by ADAR has previously been reported (42). The occurrence of both A-to-G and U-to-C substitutions can be explained by hyperediting of the positive sense cRNA as well as the negative sense vRNA, respectively. Interestingly, ADAR1 is induced by IFN and is believed to have an antiviral role during influenza infection (37). Furthermore, NS1 interacts with ADAR1, suggesting that it

447 inhibits ADAR1 function (28). Possibly, the high level of IFN induction and the absence of
448 NS1 in delNS1 infected cells resulted in more RNA hyperediting.

449 By sequence analysis of the two adapted viruses and subsequent analysis of
450 reassortant viruses generated by reverse genetics, we showed that six substitutions in the M
451 segment were responsible for the increase in delNS1^{CA2} virus titres. The increase in
452 delNS1^{CA1} viral titres was caused by substitutions in the NP, M and NS segments, where the
453 M segment was most important. Previously, adaptation to Vero cells yielded an influenza B
454 delNS1 virus with increased titres due to M1 amino acid substitution M86V (51). This is in
455 striking contrast to the many studies on the adaptation of WT virus originating from eggs or
456 clinical specimens to propagation in mammalian hosts or cell lines, which showed that
457 adaptive mutations predominantly accumulated in the HA segment or segments encoding
458 the RNA polymerase (PB1, PB2 and PA), which is assumed to be caused by adaptation to the
459 different host species (16, 29, 34, 45). This suggests that the preferential isolation of M-
460 segment mutations upon delNS1 virus adaptation compensates for the absence of the NS1
461 protein rather than the replication in a different host species. This conclusion is further
462 supported by our observation that the introduction of the M^{CA2} gene segment into a WT
463 virus (that produces NS1) does not enhance, but even reduces, viral replication.

464 Therefore, we focused on the mechanism by which the M segment mutations could
465 improve replication in the absence of NS1. The M segment encodes the M1 matrix protein
466 from unspliced M1 mRNA, whereas the M2 ion channel protein is transcribed from a spliced
467 mRNA (Fig. 2B). A second splice product, mRNA$_3$, can arise from an alternative 5' splice site
468 and encodes a hypothetical and as yet undiscovered 9 amino acid peptide (21). It was
469 previously shown that NS1 expression limits splicing, including that of the M segment-
470 derived mRNA (23, 32), resulting in a higher ratio of M1 to M2 mRNA. Furthermore, M1

471 expression is reduced in MDCK cells infected with influenza virus expressing truncated NS1
472 (8, 10). We therefore measured M1 and M2 expression in infected cells and calculated the
473 M1/M2 expression ratio, assuming that this would be dependent on the efficiency of M1
474 mRNA splicing. Indeed, cells infected with WT virus showed a higher M1/M2 expression
475 ratio than delNS1 infected cells. The M^{CA1} and M^{CA2} segments showed significantly increased
476 M1/M2 expression ratios as compared to the WT M segment, both when expressed using a
477 delNS1 virus backbone and after transfection of cells with M gene-encoding plasmids. The
478 M^{CA1} segment contains four silent mutations whereas the M^{CA2} segment contains four silent
479 and two non-silent mutations. By generating novel reassortant viruses we could show that
480 the altered M1/M2 expression ratio of $delNS1^{CA2}$ was due to the 4 silent mutations.
481 Furthermore, these silent M^{CA2} mutations caused an increase in delNS1 viral titres, although
482 not to the same extent as a segment that also contains the two non-silent M segment
483 mutations. The silent M^{CA1} and M^{CA2} mutations lay in a region that contains the major
484 determinants for M segment splicing (3). Thus it is likely that both these sets of mutations
485 lower M1 mRNA splicing efficiency in a similar manner by restoring a balance that was
486 disturbed due to the absence of NS1. Such a mechanism, aimed at restoration of M1 splicing
487 efficiency may also explain why introduction of the M^{CA2} segment into a backbone of virus
488 that produces NS1 (WT virus) reduces replication efficiency. Surprisingly, NS1 does not
489 affect the M1/M2 expression ratio in Vero cells (36). Furthermore, absence of NS1 causes
490 reduced M1 expression in MDCK but not in Vero cells (8). Taken together with our results
491 this suggests that the improved replication of delNS1 virus in Vero cells as compared to
492 MDCK cells is not only determined by the lack of an IFN response, but also by the ability of
493 Vero cells to retain efficient M segment splicing and M1 expression in the absence of NS1.

494 The major part of the increase in delNS1^{CA2} virus titre resulted from the combination
495 of M1 amino acid substitutions V97A and Y100H. As single substitutions these mutations did
496 not affect replication efficiency. Mutation V97A was previously introduced into the
497 A/WSN/33 [H1N1] strain (which is able to express NS1) and resulted in a 100-fold lower
498 virus yield (6). Residues 97 and 100 are located on the helix 6 (H6) domain, a positively
499 charged surface region between amino acids 91 to 105 of M1 (40). The influenza B M1
500 M86V mutation that enhanced delNS1 virus replication (51) is located near this region. The
501 exact mechanism by which this mutation affected viral replication was not further
502 investigated. The H6 domain has multiple functional motifs, including a nuclear localization
503 signal (NLS) between amino acids 101-105 (Fig. 2C) that binds to cellular importin-α (5).
504 Inside the nucleus, M1 binds to the vRNP complex, after which NEP can bind to the NLS of
505 M1 (1). The vRNP-M1-NEP complex can then be exported to the cytoplasm were virus
506 particles are assembled at the cell membrane (1). The localization of V97A and Y100H within
507 the H6 domain suggests that they could affect M1 binding to NEP. Furthermore, Y100H is
508 located immediately next to the NLS and may also affect importin-α binding, as described
509 earlier for a mutation next to a NLS in PB2 (29). In this manner these mutations could affect
510 M1 (and vRNP) subcellular distribution. The absence of NS1 during infection resulted in
511 decreased levels of M1 in the nucleus at late stages of the infection. This may result from
512 increased apoptosis induction by delNS1 virus as widening of the nuclear pores (11) allows
513 diffusion of vRNPs out of the nucleus (24). Amino acid changes V97A and Y100H resulted in
514 full depletion of M1 in the nucleus at 10 hpi, thus these mutations do not restore the M1
515 localization balance in delNS1 towards infection in the presence of NS1. It is therefore
516 difficult to speculate how these two mutations can cause a 50-fold increase in virus titre.

517 Interestingly, the increased viral titres of delNS1^{CA1} virus were in part due to six
518 nucleotide substitutions causing three amino acid substitutions in the NEP protein.
519 Especially substitution I76V which is located within the domain that binds to M1 (1) could -
520 similarly to the M1 mutations described above - affect vRNP nuclear export. Similar effects
521 of M1 and NEP mutations that affect their interaction were observed earlier in WT virus.
522 Mutations of NEP glutamate residues 67, 74 and 75 that bind M1, decreased vRNP content
523 of viral particles and caused morphological virion changes similar to those that occur in virus
524 particles with mutated positively charged M1 residues 95, 98, 101 and 102 that bind NEP (2,
525 6).

526 In this paper we showed that mutations in the M segment can enhance the
527 replication of delNS1 virus due to both non-silent and silent mutations, the latter
528 presumably affecting the M1 mRNA splicing efficiency. These findings contradict the
529 previous suggestion that the restricted replication of this virus in MDCK cells is primarily due
530 to the inability to inhibit the IFN response. The mutations described may have direct
531 applications as they, for example, allow the development of delNS1 based viruses with
532 improved replication efficiency, thereby making it possible to produce such a virus in other
533 cell lines than Vero cells (35) or NS1 expressing MDCK cells (46). Moreover, these mutations
534 may be combined with the G3A and C8U mutations in HA vRNA, which increased the HA
535 expression level of a live attenuated NS1 truncated influenza vaccine strain (25). However, it
536 will be necessary to determine the effect of these mutations on vaccine safety and efficacy.
537

538 **Acknowledgements**

539 This research was funded by the Impulse Veterinary Avian Influenza Research in the
540 Netherlands program of the Economic Structure Enhancement Fund.

541 The authors thank M. Vernooij, O. de Leeuw, E. de Boer, D. van Zoelen and G.
542 Tjeerdsma (CVI) for their help with the development of various assays and technical
543 assistance, and A. Dekker (CVI) for his help with the statistical data analysis.

544

545

References

1. **Akarsu, H., W. P. Burmeister, C. Petosa, I. Petit, C. W. Muller, R. W. Ruigrok, and F. Baudin.** 2003. Crystal structure of the M1 protein-binding domain of the influenza A virus nuclear export protein (NEP/NS2). Embo J **22:**4646-4655.
2. **Akarsu, H., K. Iwatsuki-Horimoto, T. Noda, E. Kawakami, H. Katsura, F. Baudin, T. Horimoto, and Y. Kawaoka.** 2011. Structure-based design of NS2 mutants for attenuated influenza A virus vaccines. Virus Res **155:**240-248.
3. **Backstrom Winquist, E., S. Abdurahman, A. Tranell, S. Lindstrom, S. Tingsborg, and S. Schwartz.** 2011. Inefficient splicing of segment 7 and 8 mRNAs is an inherent property of influenza virus A/Brevig Mission/1918/1 (H1N1) that causes elevated expression of NS1 protein. Virology **422:**46-58.
4. **Balachandran, S., P. C. Roberts, T. Kipperman, K. N. Bhalla, R. W. Compans, D. R. Archer, and G. N. Barber.** 2000. Alpha/beta interferons potentiate virus-induced apoptosis through activation of the FADD/Caspase-8 death signaling pathway. J Virol **74:**1513-1523.
5. **Boulo, S., H. Akarsu, R. W. Ruigrok, and F. Baudin.** 2007. Nuclear traffic of influenza virus proteins and ribonucleoprotein complexes. Virus Res **124:**12-21.
6. **Burleigh, L. M., L. J. Calder, J. J. Skehel, and D. A. Steinhauer.** 2005. Influenza a viruses with mutations in the m1 helix six domain display a wide variety of morphological phenotypes. J Virol **79:**1262-1270.
7. **de la Luna, S., P. Fortes, A. Beloso, and J. Ortin.** 1995. Influenza virus NS1 protein enhances the rate of translation initiation of viral mRNAs. J Virol **69:**2427-2433.
8. **Egorov, A., S. Brandt, S. Sereinig, J. Romanova, B. Ferko, D. Katinger, A. Grassauer, G. Alexandrova, H. Katinger, and T. Muster.** 1998. Transfectant influenza A viruses

with long deletions in the NS1 protein grow efficiently in Vero cells. J Virol **72:**6437-6441.

9. **Ehrhardt, C., T. Wolff, S. Pleschka, O. Planz, W. Beermann, J. G. Bode, M. Schmolke, and S. Ludwig.** 2007. Influenza A virus NS1 protein activates the PI3K/Akt pathway to mediate antiapoptotic signaling responses. J Virol **81:**3058-3067.

10. **Enami, K., T. A. Sato, S. Nakada, and M. Enami.** 1994. Influenza virus NS1 protein stimulates translation of the M1 protein. J Virol **68:**1432-1437.

11. **Faleiro, L., and Y. Lazebnik.** 2000. Caspases disrupt the nuclear-cytoplasmic barrier. J Cell Biol **151:**951-959.

12. **Ferko, B., J. Stasakova, J. Romanova, C. Kittel, S. Sereinig, H. Katinger, and A. Egorov.** 2004. Immunogenicity and protection efficacy of replication-deficient influenza A viruses with altered NS1 genes. J Virol **78:**13037-13045.

13. **Fortes, P., A. Beloso, and J. Ortin.** 1994. Influenza virus NS1 protein inhibits pre-mRNA splicing and blocks mRNA nucleocytoplasmic transport. Embo J **13:**704-712.

14. **Garcia-Sastre, A., A. Egorov, D. Matassov, S. Brandt, D. E. Levy, J. E. Durbin, P. Palese, and T. Muster.** 1998. Influenza A virus lacking the NS1 gene replicates in interferon-deficient systems. Virology **252:**324-330.

15. **Hale, B. G., R. E. Randall, J. Ortin, and D. Jackson.** 2008. The multifunctional NS1 protein of influenza A viruses. J Gen Virol **89:**2359-2376.

16. **Herfst, S., E. J. Schrauwen, M. Linster, S. Chutinimitkul, E. de Wit, V. J. Munster, E. M. Sorrell, T. M. Bestebroer, D. F. Burke, D. J. Smith, G. F. Rimmelzwaan, A. D. Osterhaus, and R. A. Fouchier.** 2012. Airborne transmission of influenza A/H5N1 virus between ferrets. Science **336:**1534-1541.

17. **Hoffmann, E., S. Krauss, D. Perez, R. Webby, and R. G. Webster.** 2002. Eight-plasmid system for rapid generation of influenza virus vaccines. Vaccine **20:**3165-3170.

18. **Hoffmann, E., J. Stech, Y. Guan, R. G. Webster, and D. R. Perez.** 2001. Universal primer set for the full-length amplification of all influenza A viruses. Arch Virol **146:**2275-2289.

19. **Kaverin, N. V., and R. G. Webster.** 1995. Impairment of multicycle influenza virus growth in Vero (WHO) cells by loss of trypsin activity. J Virol **69:**2700-2703.

20. **Kochs, G., I. Koerner, L. Thiel, S. Kothlow, B. Kaspers, N. Ruggli, A. Summerfield, J. Pavlovic, J. Stech, and P. Staeheli.** 2007. Properties of H7N7 influenza A virus strain SC35M lacking interferon antagonist NS1 in mice and chickens. J Gen Virol **88:**1403-1409.

21. **Lamb, R. A., C. J. Lai, and P. W. Choppin.** 1981. Sequences of mRNAs derived from genome RNA segment 7 of influenza virus: colinear and interrupted mRNAs code for overlapping proteins. Proc Natl Acad Sci U S A **78:**4170-4174.

22. **Le Bon, A., G. Schiavoni, G. D'Agostino, I. Gresser, F. Belardelli, and D. F. Tough.** 2001. Type i interferons potently enhance humoral immunity and can promote isotype switching by stimulating dendritic cells in vivo. Immunity **14:**461-470.

23. **Lu, Y., X. Y. Qian, and R. M. Krug.** 1994. The influenza virus NS1 protein: a novel inhibitor of pre-mRNA splicing. Genes Dev **8:**1817-1828.

24. **Ludwig, S., S. Pleschka, O. Planz, and T. Wolff.** 2006. Ringing the alarm bells: signalling and apoptosis in influenza virus infected cells. Cell Microbiol **8:**375-386.

25. **Maamary, J., N. Pica, A. Belicha-Villanueva, Y. Y. Chou, F. Krammer, Q. Gao, A. Garcia-Sastre, and P. Palese.** 2012. Attenuated influenza virus construct with enhanced hemagglutinin protein expression. J Virol **86:**5782-5790.

26. **Marazzi, I., J. S. Ho, J. Kim, B. Manicassamy, S. Dewell, R. A. Albrecht, C. W. Seibert, U. Schaefer, K. L. Jeffrey, R. K. Prinjha, K. Lee, A. Garcia-Sastre, R. G. Roeder, and A. Tarakhovsky.** 2012. Suppression of the antiviral response by an influenza histone mimic. Nature **483:**428-433.

27. **Muster, T., J. Rajtarova, M. Sachet, H. Unger, R. Fleischhacker, I. Romirer, A. Grassauer, A. Url, A. Garcia-Sastre, K. Wolff, H. Pehamberger, and M. Bergmann.** 2004. Interferon resistance promotes oncolysis by influenza virus NS1-deletion mutants. Int J Cancer **110:**15-21.

28. **Ngamurulert, S., T. Limjindaporn, and P. Auewaraku.** 2009. Identification of cellular partners of Influenza A virus (H5N1) non-structural protein NS1 by yeast two-hybrid system. Acta Virol **53:**153-159.

29. **Ping, J., L. Keleta, N. E. Forbes, S. Dankar, W. Stecho, S. Tyler, Y. Zhou, L. Babiuk, H. Weingartl, R. A. Halpin, A. Boyne, J. Bera, J. Hostetler, N. B. Fedorova, K. Proudfoot, D. A. Katzel, T. B. Stockwell, E. Ghedin, D. J. Spiro, and E. G. Brown.** 2011. Genomic and protein structural maps of adaptive evolution of human influenza a virus to increased virulence in the mouse. PLoS ONE **6:**e21740.

30. **Rae, B. P., and R. M. Elliott.** 1986. Characterization of the mutations responsible for the electrophoretic mobility differences in the NS proteins of vesicular stomatitis virus New Jersey complementation group E mutants. J Gen Virol **67:**2635-2643.

31. **Richt, J. A., and A. Garcia-Sastre.** 2009. Attenuated influenza virus vaccines with modified NS1 proteins. Curr Top Microbiol Immunol **333:**177-195.

32. **Robb, N. C., and E. Fodor.** 2011. The accumulation of influenza A virus segment 7 spliced mRNAs is regulated by the NS1 protein. J Gen Virol **93:**113-118.

33. **Robb, N. C., M. Smith, F. T. Vreede, and E. Fodor.** 2009. NS2/NEP protein regulates transcription and replication of the influenza virus RNA genome. J Gen Virol **90:**1398-1407.

34. **Roedig, J. V., E. Rapp, D. Hoper, Y. Genzel, and U. Reichl.** 2011. Impact of Host Cell Line Adaptation on Quasispecies Composition and Glycosylation of Influenza A Virus Hemagglutinin. PLoS ONE **6:**e27989.

35. **Romanova, J., B. M. Krenn, M. Wolschek, B. Ferko, E. Romanovskaja-Romanko, A. Morokutti, A. P. Shurygina, S. Nakowitsch, T. Ruthsatz, B. Kiefmann, U. Konig, M. Bergmann, M. Sachet, S. Balasingam, A. Mann, J. Oxford, M. Slais, O. Kiselev, T. Muster, and A. Egorov.** 2009. Preclinical evaluation of a replication-deficient intranasal DeltaNS1 H5N1 influenza vaccine. PLoS ONE **4:**e5984.

36. **Salvatore, M., C. F. Basler, J. P. Parisien, C. M. Horvath, S. Bourmakina, H. Zheng, T. Muster, P. Palese, and A. Garcia-Sastre.** 2002. Effects of influenza A virus NS1 protein on protein expression: the NS1 protein enhances translation and is not required for shutoff of host protein synthesis. J Virol **76:**1206-1212.

37. **Samuel, C. E.** 2011. Adenosine deaminases acting on RNA (ADARs) are both antiviral and proviral. Virology **411:**180-193.

38. **Seitz, C., T. Frensing, D. Hoper, G. Kochs, and U. Reichl.** 2010. High yields of influenza A virus in Madin-Darby canine kidney cells are promoted by an insufficient interferon-induced antiviral state. J Gen Virol **91:**1754-1763.

39. **Seitz, C., B. Isken, B. Heynisch, M. Rettkowski, T. Frensing, and U. Reichl.** 2011. Trypsin promotes efficient influenza vaccine production in MDCK cells by interfering with the antiviral host response. Appl Microbiol Biotechnol **93:**601-611.

663 40. **Sha, B., and M. Luo.** 1997. Structure of a bifunctional membrane-RNA binding
664 protein, influenza virus matrix protein M1. Nat Struct Biol **4:**239-244.
665 41. **Stasakova, J., B. Ferko, C. Kittel, S. Sereinig, J. Romanova, H. Katinger, and A.**
666 **Egorov.** 2005. Influenza A mutant viruses with altered NS1 protein function provoke
667 caspase-1 activation in primary human macrophages, resulting in fast apoptosis and
668 release of high levels of interleukins 1beta and 18. J Gen Virol **86:**185-195.
669 42. **Suspene, R., V. Petit, D. Puyraimond-Zemmour, M. M. Aynaud, M. Henry, D.**
670 **Guetard, C. Rusniok, S. Wain-Hobson, and J. P. Vartanian.** 2011. Double-stranded
671 RNA adenosine deaminase ADAR-1-induced hypermutated genomes among
672 inactivated seasonal influenza and live attenuated measles virus vaccines. J Virol
673 **85:**2458-2462.
674 43. **Talon, J., M. Salvatore, R. E. O'Neill, Y. Nakaya, H. Zheng, T. Muster, A. Garcia-**
675 **Sastre, and P. Palese.** 2000. Influenza A and B viruses expressing altered NS1
676 proteins: A vaccine approach. Proc Natl Acad Sci U S A **97:**4309-4314.
677 44. **Tan, S. L., and M. G. Katze.** 1999. The emerging role of the interferon-induced PKR
678 protein kinase as an apoptotic effector: a new face of death? J Interferon Cytokine
679 Res **19:**543-554.
680 45. **Tseng, Y. F., A. Y. Hu, M. L. Huang, W. Z. Yeh, T. C. Weng, Y. S. Chen, P. Chong, and**
681 **M. S. Lee.** 2011. Adaptation of high-growth influenza H5N1 vaccine virus in Vero
682 cells: implications for pandemic preparedness. PLoS ONE **6:**e24057.
683 46. **van Wielink, R., M. M. Harmsen, D. E. Martens, B. P. Peeters, R. H. Wijffels, and R.**
684 **J. Moormann.** 2011. MDCK cell line with inducible allele B NS1 expression
685 propagates delNS1 influenza virus to high titres. Vaccine **29:**6976-6985.

686 47. **van Wielink, R., H. C. Kant-Eenbergen, M. M. Harmsen, D. E. Martens, R. H.**
687 **Wijffels, and J. M. Coco-Martin.** 2011. Adaptation of a Madin-Darby canine kidney
688 cell line to suspension growth in serum-free media and comparison of its ability to
689 produce avian influenza virus to Vero and BHK21 cell lines. J Virol Methods **171:**53-
690 60.
691 48. **Wacheck, V., A. Egorov, F. Groiss, A. Pfeiffer, T. Fuereder, D. Hoeflmayer, M. Kundi,**
692 **T. Popow-Kraupp, M. Redlberger-Fritz, C. A. Mueller, J. Cinatl, M. Michaelis, J.**
693 **Geiler, M. Bergmann, J. Romanova, E. Roethl, A. Morokutti, M. Wolschek, B. Ferko,**
694 **J. Seipelt, R. Dick-Gudenus, and T. Muster.** 2010. A novel type of influenza vaccine:
695 safety and immunogenicity of replication-deficient influenza virus created by
696 deletion of the interferon antagonist NS1. J Infect Dis **201:**354-362.
697 49. **Wang, Z., N. C. Robb, E. Lenz, T. Wolff, E. Fodor, and S. Pleschka.** 2010. NS
698 reassortment of an H7-type highly pathogenic avian influenza virus affects its
699 propagation by altering the regulation of viral RNA production and antiviral host
700 response. J Virol **84:**11323-11335.
701 50. **Wolschek, M., E. Samm, H. Seper, S. Sturlan, I. Kuznetsova, C. Schwager, A.**
702 **Khassidov, C. Kittel, T. Muster, A. Egorov, and M. Bergmann.** 2011. Establishment of
703 a chimeric, replication-deficient influenza A virus vector by modulation of splicing
704 efficiency. J Virol **85:**2469-2473.
705 51. **Wressnigg, N., D. Voss, T. Wolff, J. Romanova, T. Ruthsatz, I. Mayerhofer, M.**
706 **Reiter, S. Nakowitsch, J. Humer, A. Morokutti, T. Muster, A. Egorov, and C. Kittel.**
707 2009. Development of a live-attenuated influenza B DeltaNS1 intranasal vaccine
708 candidate. Vaccine **27:**2851-2857.

52. **Wurzer, W. J., O. Planz, C. Ehrhardt, M. Giner, T. Silberzahn, S. Pleschka, and S. Ludwig.** 2003. Caspase 3 activation is essential for efficient influenza virus propagation. Embo J **22:**2717-2728.

53. **Ye, Z., D. Robinson, and R. R. Wagner.** 1995. Nucleus-targeting domain of the matrix protein (M1) of influenza virus. J Virol **69:**1964-1970.

54. **Yoneyama, M., W. Suhara, Y. Fukuhara, M. Sato, K. Ozato, and T. Fujita.** 1996. Autocrine amplification of type I interferon gene expression mediated by interferon stimulated gene factor 3 (ISGF3). J Biochem **120:**160-169.

55. **Zhirnov, O. P., and H. D. Klenk.** 2007. Control of apoptosis in influenza virus-infected cells by up-regulation of Akt and p53 signaling. Apoptosis **12:**1419-1432.

56. **Zhirnov, O. P., T. E. Konakova, W. Garten, and H. Klenk.** 1999. Caspase-dependent N-terminal cleavage of influenza virus nucleocapsid protein in infected cells. J Virol **73:**10158-10163.

57. **Zhirnov, O. P., T. E. Konakova, T. Wolff, and H. D. Klenk.** 2002. NS1 protein of influenza A virus down-regulates apoptosis. J Virol **76:**1617-1625.

Figure legends

Fig. 1. Replication of delNS1 virus adapted to growth on MDCK-SFS cells. Maximum infectious virus titre during each passage step of the second delNS1 adaptation experiment (A). Replication kinetics of the two adapted delNS1^{CA1} and delNS1^{CA2} virus strains in comparison to WT and parental delNS1^{EA} virus after infection of MDCK-SFS (B) or Vero (C) cells at MOI 0.01. Geometric mean titres and 95% confidence interval of the mean of virus infections performed in triplicate are presented.

Fig. 2. Nucleotide substitutions in M-gene segments of adapted delNS1 viruses. (A) Sequence analysis of delNS1^{CA2} showing the simultaneous accumulation of six U-to-C substitutions (indicated by arrows) in the M segment vRNA between position 277-325 from passages 3 to 5 on MDCK-SFS cells. Double peaks are visible at passage 4 and 5. Note that in the electropherograms U is shown as T. (B) Schematic overview of the M segment mRNAs, with the locations of the adaptive M^{CA1} and M^{CA2} mutations and splicing products M2 mRNA and mRNA3. Open reading frames are indicated by thick bars. (C) Nucleotide sequences of the M^{CA1} and M^{CA2} regions shown in panel B, including the amino acid sequence of M^{CA2}, where dots indicate sequence identity of M1^{CA2} to M1^{WT}. The square box indicates the location of the NLS in M1, with positively charged (+) amino acids (53). The arrow indicates the location of the adaptive mutation in influenza B M1 protein found earlier (51). The amino acid sequence of M1^{CA1} is not shown since it is identical to M1^{WT} (i.e. all mutations were silent).

Fig. 3. Comparison of infectious virus titres 3 d after infection of MDCK-SFS cells with the cell-adapted or the various reassortant virus strains (MOI 0.01). (A) Titres of delNS1

reassortant viruses made with original delNS1 plasmids (not-filled), or plasmids containing single or multiple mutations originating from the adapted virus strains delNS1^{CA1} (filled, marked 1) and delNS1^{CA2} (filled, marked 2). (B) Titres of delNS1 reassortant viruses containing one or more of the delNS1^{CA2} M segment mutations and of WT reassortant virus containing the M^{CA2} mutations. In both panels, geometric mean titres and 95% confidence interval of the mean are presented of triplicate measurements.

Fig. 4. Effect of delNS1 virus adaptation on IFN-β and apoptosis induction. IFN induction in MDCK-SFS cells infected with either WT, delNS1, delNS1^{CA1} or delNS1^{CA2} virus, or mock infected (A), and delNS1:M^{CA1}, delNS1:M^{CA2} or delNS1:M$^{CA2.3}$ virus (B) was measured with an IFN-β dependent luciferase reporter construct and corrected for transfection efficiency with Renilla luciferase. (C) Induction of apoptosis in MDCK-SFS cells infected with either WT, delNS1, delNS1^{CA1} or delNS1^{CA2} virus, or mock infected. Apoptosis induction was assessed by measuring the activity of caspase 3 and 7. Geometric mean activities and 95% confidence interval of the mean are presented of experiment performed in triplicate.

Fig. 5. Western blot analysis of M1 and M2 protein expression 10 h after infection of MDCK-SFS cells (A) or 48 h after transient transfection of HEK293T cells (C) with plasmid (Table 1) containing either the WT M segment (pHW197), the mutated M^{CA1} or M^{CA2} segments (pROM36 and pROM35), or the M segment containing one or more delNS1^{CA2} mutations (pROM51-54). M1 and M2 protein levels of three independent experiments were quantified using phosphorimager densitometry. The M1/M2 ratio for each virus (B) or plasmid (D) is shown as the mean and 95% confidence interval of the mean. Lanes 1-4 and lanes 5-8 in panel A originated from two different blots.

774

775 **Fig. 6.** Subcellular localization of M1 protein. MDCK-SFS cells were infected with WT, delNS1
776 and delNS1:$M^{CA2.3}$ virus at high MOI in triplicate. Then, cytoplasm and nucleoplasm fractions
777 were prepared at 6 hpi and 10 hpi and M1 protein was quantified by Western blot analysis.
778 Panel (A) shows one representative Western blot. Tubulin (Tub) and lamin A/C (Lam) were
779 used as cytoplasm and nucleoplasm specific controls, respectively. The isolations were
780 successful as no tubulin was observed in the nucleoplasm isolates (lane 1-6) and no lamin
781 A/C was observed in the cytoplasm isolates (lane 8-13). The cytoplasmic isolate of WT virus
782 at 6 hpi was used as a source of tubulin in lane 7 whereas the nucleoplasmic isolate of WT
783 virus at 6 hpi was used as a source of lamin A/C in lane 14. Nuclear isolates show aspecific
784 staining by the tubulin antibody (lane 1-6), which is not present in the cytoplasmic control
785 (lane 7). (B) M1 protein levels were quantified by phosphorimager densitometry using
786 tubulin and lamin A/C, respectively, as controls to compensate for the isolation efficiency.
787 The ratio of corrected nuclear M1 ($M1_n$) to corrected cytoplasmic M1 ($M1_c$) was used to
788 determine changes in the distribution of M1 and is shown as the mean and 95% confidence
789 interval of the mean at 6 hpi (empty bars) and 10 hpi (filled bars).

790

791 Tables:

792 Table 1. pHW2000-derived plasmids encoding mutant gene segments from cell-adapted

793 delNS1 viruses.

Plasmid	Segment	Nucleotide substitutions	Amino acid substitutions[a]
pROM34	HA^{CA1}	U796C	F257L
pROM33	HA^{CA2}	C1326A	None
pROM16	NP^{CA1}	A1381G	R446G
pROM36	M^{CA1}	U640C, U643C, U652C, U688C	None
pROM35	M^{CA2}	U277C, U298C, U315C, U316C, U323C, U325C	V97A, Y100H
pROM51	$M^{CA2.1}$	U315C	V97A
pROM52	$M^{CA2.2}$	U323C	Y100H
pROM53	$M^{CA2.3}$	U315C, U323C	V97A, Y100H
pROM54	$M^{CA2.4}$	U277C, U298C, U316C, U325C	None
pROM13	NS^{CA1}	A148G, A173G, A179G, A180G, A248G, A252G	Y41C, M52V, I76V

794 [a] *Amino acid positions are relative to methionine in the open reading frame.*

795
796

797 Table 2. Mutations in egg adapted delNS1^{EA} and cell adapted delNS1^{CA1} and delNS1^{CA2} virus

798 strains.

Gene segment	Nucleotide position[a]	Nucleotide substitution[b] delNS1^{EA}	delNS1^{CA1}	delNS1^{CA2}	Amino acid substitution[b]
PB1 (S2)	798	-	G to U	-	-
	1953	A to U 50%[c]	A to U	A to U	-
	2133	U to C 50%[c]	U to C	U to C	-
HA (S4)	796	-	U to C	-	F257L
	1326 (1338)	C to A 50%[c]	-	C to A	-
NP (S5)	1381	-	A to G	-	R446G
M (S7)	277	-	-	U to C	-
	298	-	-	U to C	-
	315	-	-	U to C	V97A
	316	-	-	U to C	-
	323	-	-	U to C	Y100H
	325	-	-	U to C	-
	640	-	U to C	-	-
	643	-	U to C	-	-
	652	-	U to C	-	-
	688	-	U to C	-	-
NS (S8)	148 (620)	-	A to G	-	Y41C
	173 (645)	-	A to G	-	-
	179 (651)	-	A to G	-	-
	180 (652)	-	A to G	-	M52V
	248 (720)	-	A to G	-	-
	252 (724)	-	A to G	-	I76V

799 *[a] Numbering refers to nucleotide positions in the vRNA template [GenBank accession no:*

800 *EF467819 (PB1), DQ407519 (HA), EF467822 (NP), EF190985 (M), AF389122 (NS)]. Note that*

801 *the numbering of the HA and NS mutations refers to the recombinant gene segments (46).*

802 *The numbering in line with the Genbank sequences is placed between brackets.*

803 *[b] Substitutions as compared to sequence of plasmid used for initial delNS1 virus generation.*

804 *– No substitution.*

805 *[c] Presence of a second nucleotide sequence within the seed virus.*

806

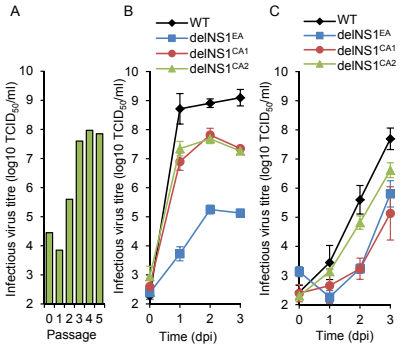

Figure 1: Role of M segment in delNS1 influenza replication. R. van Wielink et al.

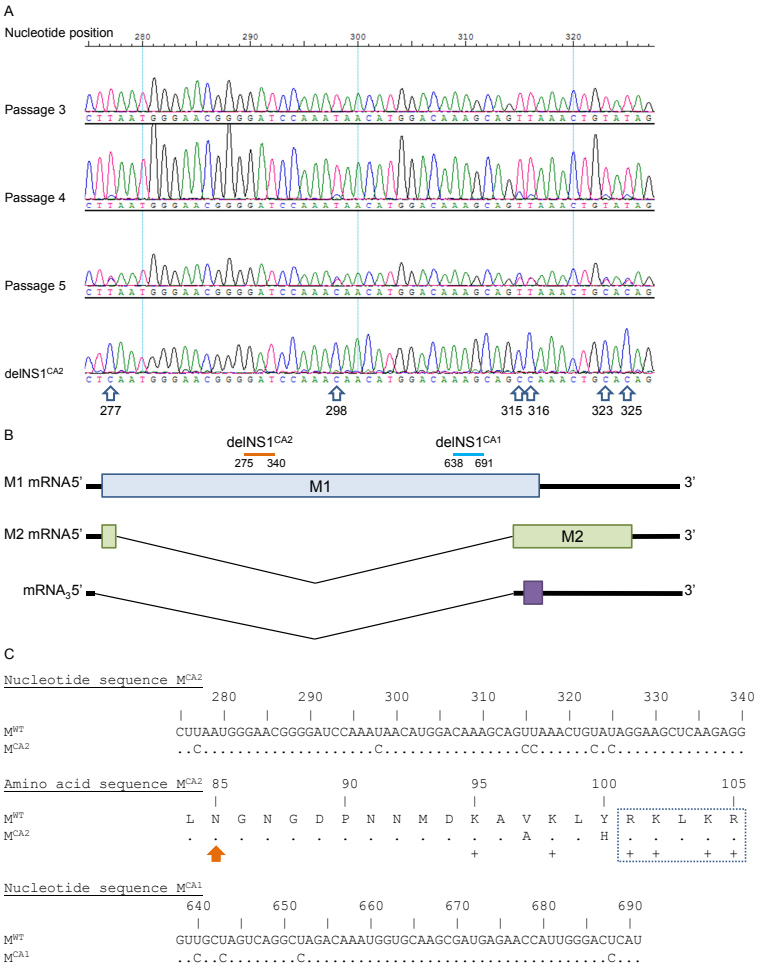

Figure 2: Role of M segment in delNS1 influenza replication. R. van Wielink et al.

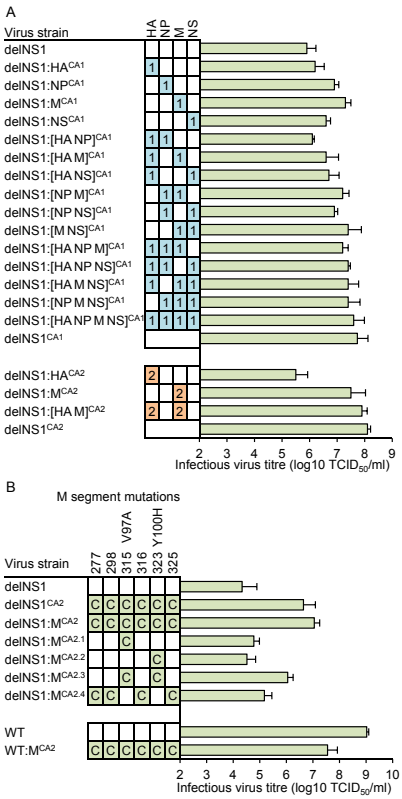

Figure 3: Role of M segment in delNS1 influenza replication. R. van Wielink et al.

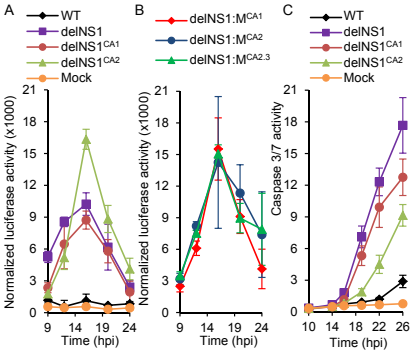

Figure 4: Role of M segment in delNS1 influenza replication. R. van Wielink et al.

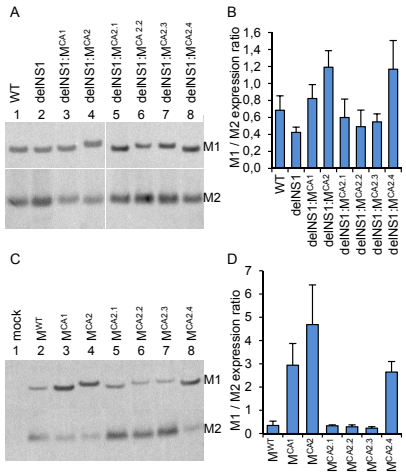

Figure 5: Role of M segment in delNS1 influenza replication. R. van Wielink et al.

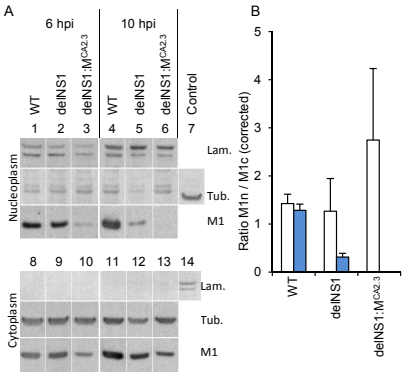

Figure 6: Role of M segment in delNS1 influenza replication. R. van Wielink et al.